Available online at www.sciencedirect.com
ScienceDirect
Journal of Organometallic Chemistry 692 (2007) 4708–4716
Journal of Organometallic Chemistry
www.elsevier.com/locate/jorganchem

Insertion vs. site epimerization with singly-bridged and doubly-bridged metallocene polymerization catalysts

Stephen A. Miller

Department of Chemistry, Texas A&M University, College Station, TX 77843-3255, United States

Received 2 April 2007; received in revised form 8 June 2007; accepted 8 June 2007
Available online 29 June 2007

This paper is dedicated to Professor Dr. Gerhard Erker on the occasion of his 60th birthday.

Abstract

A statistical model has been employed to determine the unidirectional site epimerization probability, ε, during propylene polymerization with the following C_1-symmetric metallocene precatalysts activated with MAO (MAO = methylaluminoxane): doubly-bridged *rac*-(1,2-$SiMe_2$)$_2$\{η^5-C_5H_2-4-(CHMe(CMe_3))\}\{η^5-C_5H-3,5-($CHMe_2$)$_2$\}$ZrCl_2$ (**1**) and (1,2-$SiMe_2$)$_2$\{η^5-C_5H_2-4-(1*R*,2*S*,5*R*-menthyl)\}\{η^5-C_5H-3,5-($CHMe_2$)$_2$\}$ZrCl_2$ (**2**); and singly-bridged Me_2C(3-(2-adamantyl)-C_5H_3)($C_{13}H_8$)$ZrCl_2$ (**3**) and Me_2Si(3-(2-adamantyl)-C_5H_3)($C_{13}H_8$)$ZrCl_2$ (**4**). For **1**/MAO a steep tacticity dependence on monomer concentration was found, as ε increased from 0.114 to 0.909 as [C_3H_6] decreased from 12.5 M to 0.5 M; similarly, ε increased for **2**/MAO from 0.177 to 0.709. For **3**/MAO, ε was moderately responsive to an increase in polymerization temperature, as ε increased from 0.000 to 0.485 from T_p = 0–90 °C ([C_3H_6] = 1.1 M). Similarly, ε increased for **4**/MAO from 0.709 to 0.913 from T_p = 0–40 °C; at higher temperatures, bidirectional site epimerization was implicated.

Keywords: Metallocene catalysts; Polypropylene; Tacticity; Stereochemical model; *ansa*-Metallocene; Doubly-bridged metallocene

1. Introduction

Metallocene polymerization catalysts are well appreciated for their steric tunability to produce poly(α-olefins) having a wide variety of stereochemical structures [1]. The interpretation of α-olefin polymer tacticities through stereochemical statistical models has long been the subject of intense research [2]. Despite their idealized nature and variable applicability to real polymerization systems, such models are indispensable tools for understanding the fundamental processes that occur at the transition metal during polymerization [3].

Herein is reported the application of a statistical model to doubly-bridged [4] and singly-bridged [5] C_1-symmetric *ansa*-metallocene/MAO (MAO = methylaluminoxane) polymerization systems (Fig. 1). The model employed is derived from previous models developed by Farina et al. [6], by Collins et al. [7], and by Randall et al. [8]. However, this appears to be the first attempt to quantify the site epimerization process with doubly-bridged metallocene polymerization catalysts, thereby providing a direct mechanistic comparison with the behavior of singly-bridged metallocenes.

Monomer approach can occur at either one of two vacant sites of an active metallocene catalyst (Fig. 2). The modified Rooney–Green mechanism [9] mandates alternating employment of these two sites for the bimolecular propagation steps. A unimolecular site epimerization process, however, can compete with the bimolecular insertion process and becomes stereochemically important when the two sites are not homotopic—that is, when the precatalyst lacks a C_2-axis of symmetry. As a result, the alternating mechanism can yield to the site epimerization mechanism [10] and the relative frequency of these events can be quantified [11].

E-mail address: samiller@mail.chem.tamu.edu

0022-328X/$ - see front matter © 2007 Elsevier B.V. All rights reserved.
doi:10.1016/j.jorganchem.2007.06.043

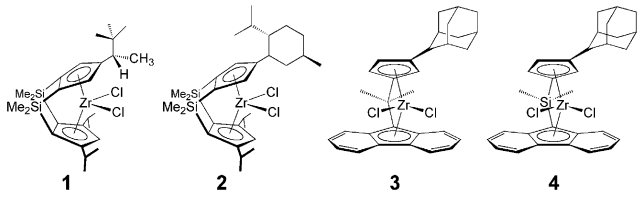

Fig. 1. Doubly-bridged and singly-bridged C_1-symmetric metallocene catalyst precursors **1**–**4**.

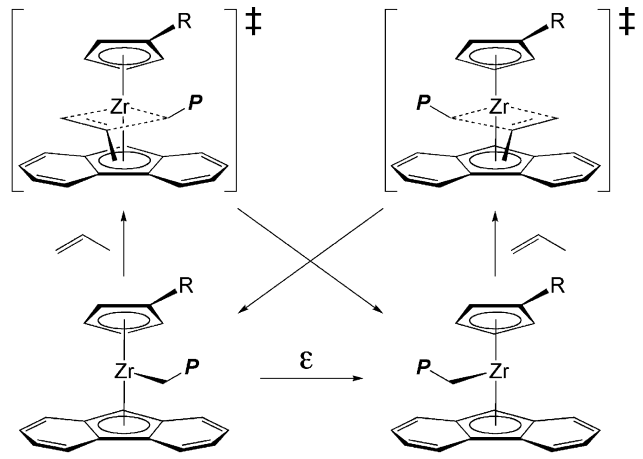

Fig. 2. Unidirectional site epimerization (ε) can complete with an otherwise regular migratory insertion process, which employs the two coordination sites in an alternating fashion (**P** = polymer chain).

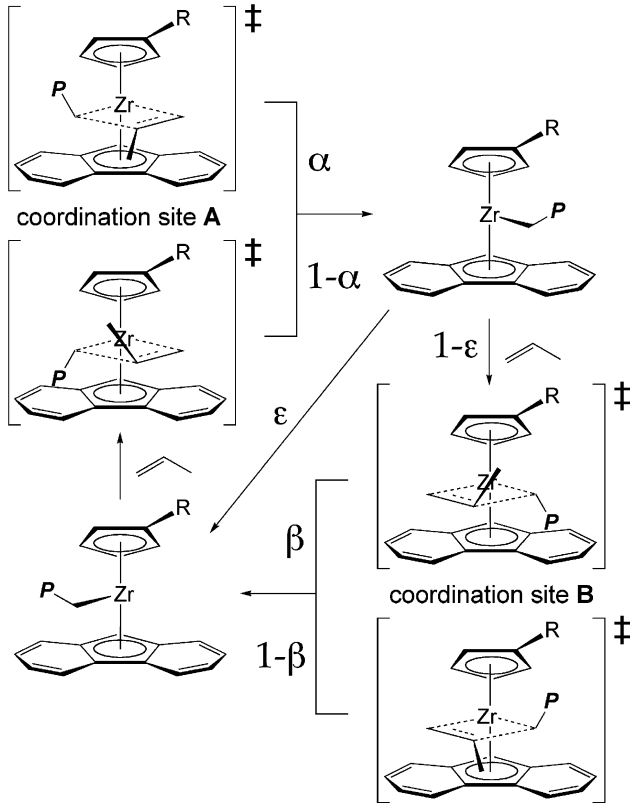

Fig. 3. The unidirectional site epimerization model employs two stereochemical parameters (α and β) and the unidirectional site epimerization parameter (ε). The stereoselectivity parameter α applies to the more stereoselective site while the stereoselectivity parameter β applies to the less stereoselective site (**P** = polymer chain).

2. Results and discussion

2.1. The unidirectional site epimerization model

Fig. 3 depicts coordination site A as the more stereoselective site and coordination site B as the less stereoselective site of a generic C_1-symmetric metallocene. The alternating mechanism requires an ABABA or BABAB site employment for creation of a pentad. However, if the growing polymer chain is allowed to move away from the bulky R substituent—but not towards it—prior to monomer insertion, such a unidirectional site epimerization [12] permits eleven additional site sequences. The probabilities of insertion at site A and site B can be calculated in terms of ε, the unidirectional site epimerization probability. In addition to the parameter ε, the unidirectional site epimerization model has two other independent parameters, α and β, which describe the enantioselectivity of site A and site B, respectively. Here, these are defined such that a value of 1.0 for α and a value of 1.0 for β correspond to the same absolute sense of enantiofacial selectivity at each site. See the Supplementary material for full details.

2.2. Application of the unidirectional site epimerization model to doubly-bridged metallocenes

Bercaw et al. have previously reported propylene polymerization results obtained with C_1-symmetric, doubly-bridged metallocenes (**1** and **2**, Fig. 1) [4]. With *rac*-(1,2-$SiMe_2$)$_2${η^5-C_5H_2-4-(CHMe(CMe_3))}{η^5-C_5H-3,5-($CHMe_2$)$_2$}$ZrCl_2$/MAO (**1**/MAO), a steep tacticity dependence on monomer concentration was found, as the system gradually changes from syndioselective to isoselective with decreasing monomer concentration. In liquid propylene relatively syndiotactic polypropylene is obtained having $[r] = 79.8\%$ for $T_p = 20$ °C, while under dilute monomer conditions of 0.5 M propylene in toluene, isotactic polypropylene is obtained with $[m] = 88.5\%$ for $T_p = 25$ °C. Table 1 tabulates the polymerization data obtained with **1**/MAO [4b].

A least squares fit [13] was performed on the pentad distribution for entry 1 (liquid monomer, $T_p = 20$ °C, see Table 1). This established the enantiofacial selectivity parameters and the calculated site epimerization parameter for this catalyst in liquid propylene at 20 °C. The parameter α was determined to be 0.991 while β was determined to be 0.166. These numbers suggest that catalyst **1**/MAO has one highly enantioselective site (99.1%) and one moderately enantioselective site having the opposite enantiofacial selectivity (83.4%). The parameter ε was found to be 0.114, meaning that the less selective site (site B) is skipped 11.4% of the time because unimolecular site epimerization competes with bimolecular insertion at that point in the catalytic cycle.

Table 1
Polymerization data for catalyst systems **1**–**4**/MAO

Entry	Catalyst/MAO	$[C_3H_6]$ (M)[a]	T_p (°C)	[*m*] (%)	[*r*] (%)	T_m (°C)[b]	Reference
1	**1**	12.5	20	20.2	79.8	102	[4b, Entry 25]
2	**1**	4.6	25	39.8	60.4	n.o.	[4b, Entry 32]
3	**1**	3.4	25	50.5	49.5	n.d.	[4b, Entry 31]
4	**1**	2.1	25	62.0	38.0	n.d.	[4b, Entry 30]
5	**1**	0.8	25	86.7	13.3	108	[4b, Entry 29]
6	**1**	0.5	25	87.8	12.1	n.d.	[4b, Entry 28]
7	**2**	12.5	20	25.9	74.1	n.o.	[4b, Entry 26]
8	**2**	4.6	25	24.8	75.2	n.o.	[4b, Entry 37]
9	**2**	3.4	25	29.4	70.6	n.d.	[4b, Entry 36]
10	**2**	2.1	25	44.6	55.3	106	[4b, Entry 35]
11	**2**	0.8	25	53.0	47.0	80	[4b, Entry 34]
12	**2**	0.5	25	60.0	39.8	n.d.	[4b, Entry 33]
13	**3**	1.1	0	60.2	39.9	n.o.	[5a, Entry 13]
14	**3**	1.1	20	59.7	40.2	n.o.	[5a, Entry 14]
15	**3**	1.1	40	60.6	39.4	n.o.	[5a, Entry 15]
16	**3**	1.1	60	62.1	37.9	n.o.	[5a, Entry 16]
17	**3**	1.1	75	67.3	32.7	n.o.	[5a, Entry 17]
18	**3**	1.1	90	71.6	28.4	n.o.	[5a, Entry 18]
19	**4**	1.1	0	79.3	20.7	77	[5a, Entry 19]
20	**4**	1.1	20	87.8	12.0	118	[5a, Entry 20]
21	**4**	1.1	40	88.5	11.5	127	[5a, Entry 21]
22	**4**	1.1	60	84.4	15.6	123	[5a, Entry 22]
23	**4**	1.1	80	83.2	16.8	110	[5a, Entry 23]

[a] 12.5 M $[C_3H_6]$ corresponds to liquid monomer. 1.1 M $[C_3H_6]$ corresponds to 3 mL propylene in 30 mL toluene.
[b] n.d. = not determined; n.o. = no melting temperature observed by DSC.

As the monomer concentration is decreased, this unimolecular site epimerization is able to compete more effectively with bimolecular propagation. As the concentration decreases (12.5, 4.6, 3.4, 2.1, 0.8, 0.5 M), the site epimerization probability, ε, increases: 0.114, 0.406, 0.578, 0.718, 0.910, 0.909. At the lowest monomer concentration investigated, an insertion at site A is followed by a site epimerization 91% of the time, while it is followed by successful insertion at site B only 9% of the time.

For this analysis, an assumption is made that α and β are intrinsic to the organometallic catalyst and do not vary significantly with concentration. Indeed, allowing α, β, and ε to vary independently provides satisfactorily similar results for those pentad distributions that contain significant fractions of eight or nine pentads (entries 2–4). Without this assumption, the parameters obtained for entries 5 and 6 can be varied considerably with only small changes in the RMS error. This arises because deviations in the parameter β become less important as ε approaches unity. Table 2 provides the numerical results of the statistical fits, and Fig. 4 provides a visual comparison between the observed ^{13}C NMR pentad distributions [2d,14] and those calculated by the unidirectional site epimerization model.

If the enantiofacial selectivity parameters α and β remain constant for **1**/MAO and epsilon is extrapolated to $\varepsilon = 0$ (no site epimerization), the model yields values

Table 2
Unidirectional site epimerization model applied to **1**/MAO[a]

Entry	1		2		3		4		5		6	
	obs	calc	obs	calc	obs	calc	obs	calc	obs	calc	obs	calc
[*mmmm*]	1.3	2.1	9.9	7.1	17.7	15.4	29.3	28.6	65.5	65.5	65.6	65.1
[*mmmr*]	4.4	4.5	11.6	10.6	15.0	14.8	16.6	16.9	13.0	11.7	14.4	11.8
[*rmmr*]	4.0	4.8	3.7	4.2	3.3	3.6	3.2	2.5	0.9	0.5	0.5	0.5
[*mmrr*]	14.4	13.9	18.9	18.5	19.9	21.6	18.1	21.6	12.8	12.6	13.6	12.7
[*mmrm*] + [*rrmr*]	6.6	7.0	10.3	13.0	9.1	10.7	7.3	6.9	0.9	1.4	0.5	1.4
[*mrmr*]	0.0	0.3	0.0	0.5	0.0	0.5	0.5	0.5	0.9	0.2	0.5	0.2
[*rrrr*]	49.5	49.3	23.9	22.7	14.6	11.8	7.2	5.5	0.9	0.7	0.5	0.7
[*rrrm*]	17.5	15.4	16.2	15.7	12.0	11.5	8.8	6.9	0.9	1.2	0.5	1.2
[*mrrm*]	2.3	2.6	5.7	7.7	8.3	10.2	9.1	10.6	4.2	6.3	3.8	6.3
[*m*]	20.2	22.1	39.8	37.8	50.5	50.2	62.0	62.5	86.7	84.8	87.8	84.7
[*r*]	79.8	77.9	60.4	62.2	49.5	49.8	38.0	37.5	13.3	15.2	12.1	15.3
ε		0.114		0.406		0.578		0.718		0.910		0.909
RMS error		0.854		1.591		1.603		1.584		0.876		1.313

[a] The parameters α (0.991) and β (0.166) are determined by RMS minimization of entry 1 and are maintained at these values for application to entries 2–6.

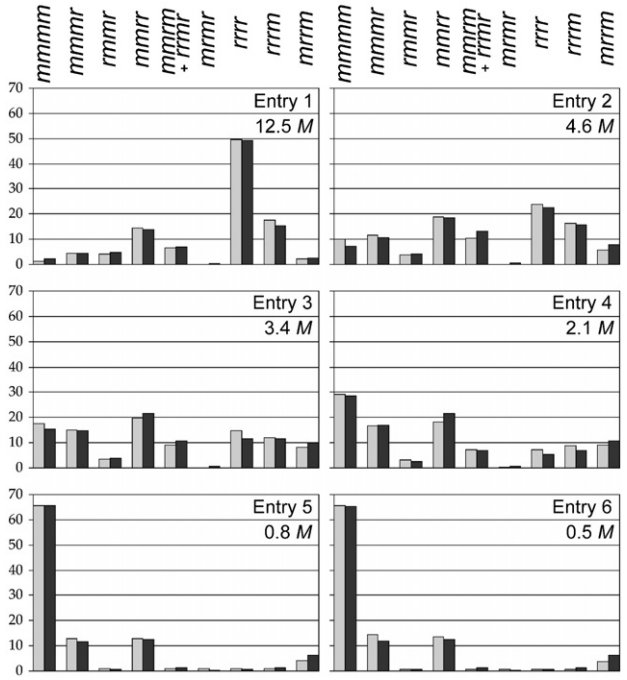

Fig. 4. Observed (light) vs. calculated (dark) pentad distributions for the unidirectional site epimerization model applied to **1**/MAO (Table 2, entries 1–6).

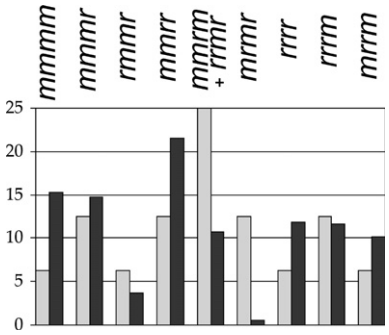

Fig. 5. Comparison of the pentad distribution for perfectly atactic polypropylene (light) to that predicted for **1**/MAO with $[m] = [r] = 50\%$ (dark).

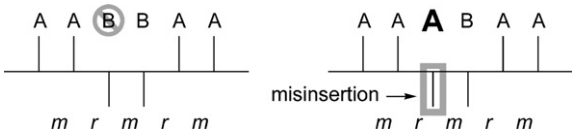

Fig. 6. Since consecutive insertions at site B are forbidden under the unidirectional site epimerization model, the *mrmr* pentad implies an enantiofacial misinsertion at the more stereoselective site A.

of $[r] = 82.8\%$ and $[rrrr] = 62.4\%$. This suggests that even under ideal polymerization conditions, only modestly syndiotactic polypropylene could be obtained. Similarly, if epsilon is extrapolated to $\varepsilon = 1.0$ (exclusive site epimerization), the model yields values of $[m] = 98.2\%$ and $[mmmm] = 95.6\%$. In principle, considerably isotactic polypropylene could be obtained with **1**/MAO. In practice, such conditions (low monomer concentration and high temperature) might effect low molecular weight polymers and chain epimerizations [15].

If epsilon is interpolated until $[r] = [m] = 50\%$, the model predicts $\varepsilon = 0.576$. With this epsilon value, **1**/MAO is more likely to site epimerize than not, site A is employed 70.2% $(=1/(2-\varepsilon))$ of the time, and site B is employed 29.8% $(=(1-\varepsilon)/(2-\varepsilon))$ of the time. Interestingly, this catalyst system is unable to produce atactic polypropylene, as $[rrrr] = 11.9\%$ and $[mmmm] = 15.2\%$ for this polymer. The pentad distribution for this polymer is compared with that for perfectly atactic polypropylene ($[rrrr] = [mmmm] = 6.25\%$) in Fig. 5. One striking difference is that the calculated *mrmr* peak (0.5%) is almost absent. This absence is readily understood by analyzing the most likely route to form the *mrmr* pentad, as depicted in Fig. 6. Since the probability of employing a site sequence with two consecutive B sites is zero for the unidirectional site epimerization model, the only way to create the *mrmr* pentad is for an

Table 3
Unidirectional site epimerization model applied to **2**/MAO[a]

Entry	7		8		9		10		11		12	
	obs	calc	obs	calc	obs	calc	obs	calc	obs	calc	obs	calc
[*mmmm*]	3.3	2.0	1.6	2.8	4.3	3.4	11.5	9.6	18.6	17.5	26.3	25.6
[*mmmr*]	4.5	4.8	6.8	6.1	8.1	7.0	12.9	12.3	15.9	15.4	15.3	16.7
[*rmmr*]	6.0	4.3	2.6	4.2	3.9	4.2	4.4	4.1	2.6	3.5	3.8	2.8
[*mmrr*]	12.9	13.0	16.1	14.1	14.7	14.9	19.5	19.8	21.5	21.7	17.2	21.7
[*mmrm*] + [*rrmr*]	11.4	10.3	11.4	12.4	11.4	13.2	12.1	13.1	9.4	10.3	8.9	7.8
[*mrmr*]	0.0	0.5	0.0	0.5	0.0	0.6	0.0	0.8	0.8	0.8	3.0	0.7
[*rrrr*]	45.4	45.5	38.3	38.2	34.4	34.2	18.8	17.1	11.2	9.8	7.0	6.2
[*rrrm*]	13.7	16.4	19.3	17.2	17.2	17.2	13.3	14.2	11.8	10.5	8.5	7.7
[*mrrm*]	2.8	3.2	3.8	4.4	5.9	5.2	7.4	9.0	8.2	10.5	9.7	10.7
[*m*]	25.9	23.0	24.8	26.7	29.4	28.9	44.6	42.8	53.0	52.8	60.1	60.3
[*r*]	74.1	77.0	75.2	73.3	70.6	71.1	55.4	57.2	47.0	47.2	39.9	39.7
ε		0.177		0.248		0.289		0.504		0.629		0.709
RMS error		1.234		1.281		0.854		1.161		1.144		1.910

[a] The parameters α (0.987) and β (0.141) are determined by RMS minimization of entry 7 and are maintained at these values for application to entries 8–12.

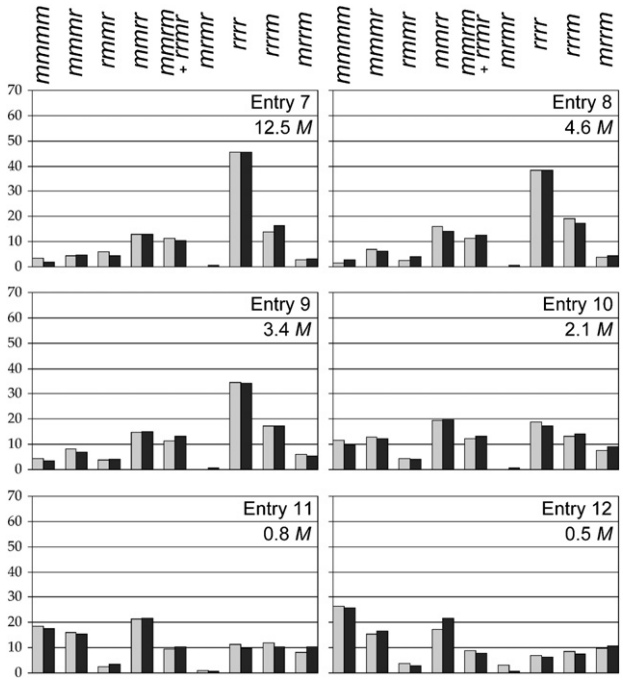

Fig. 7. Observed (light) vs. calculated (dark) pentad distributions for the unidirectional site epimerization model applied to **2**/MAO (Table 3, entries 7–12).

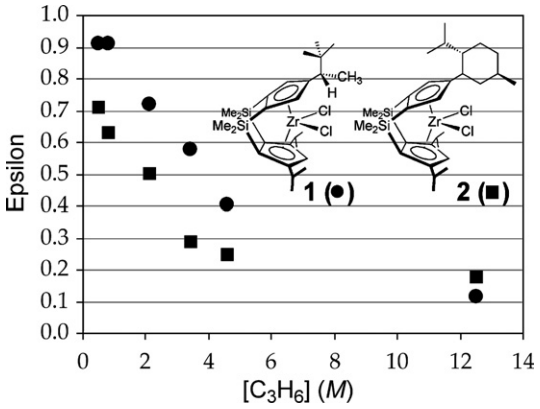

Fig. 8. The site epimerization parameter ε varies as a function of propylene concentration for **1**/MAO (circles) and **2**/MAO (squares) at 25 °C.

enantiofacial misinsertion to occur at site A, which is 99.1% selective. Indeed, this pentad is virtually absent in every polymer from **1**/MAO [16].

An analysis with similar results can be performed on polypropylenes obtained from (1,2-$SiMe_2$)$_2${η^5-C_5H_2-4-(1*R*,2*S*,5*R*-menthyl)}{η^5-C_5H-3,5-$(CHMe_2)_2$}$ZrCl_2$/MAO (**2**/MAO) over a range of monomer concentrations (entries 7–12). The least squares minimization of entry 7 (Table 3) provides the following parameters: $\alpha = 0.987$; $\beta = 0.141$; $\varepsilon = 0.177$. With fixed values of α and β, the unidirectional site epimerization parameter increases with decreasing monomer concentration. As the concentration decreases (12.5, 4.6, 3.4, 2.1, 0.8, 0.5 M) the site epimerization probability, ε, increases: 0.177, 0.248, 0.289, 0.504, 0.629, 0.709. The observed and calculated pentad distributions for **2**/MAO can be compared in Fig. 7. Fig. 8 plots the unidirectional site epimerization parameter, ε, as a function of monomer concentration for both **1**/MAO and **2**/MAO with a polymerization temperature of 25 °C.

2.3. Application of the unidirectional site epimerization model to singly-bridged metallocenes

The singly-bridged metallocene catalyst Me_2C(3-(2-adamantyl)-C_5H_3)($C_{13}H_8$)$ZrCl_2$/MAO (**3**/MAO) has been subjected to a series of propylene polymerizations conducted at increasing polymerization temperatures [5a]. A least squares fit of the unidirectional site epimerization model to entry 13 ($[C_3H_6] = 1.1$ M, $T_p = 0$ °C) produces the following parameters for this catalyst: $\alpha = 0.974$, $\beta = 0.599$ and $\varepsilon = 0.000$ (Table 4). This indicates that both sites of the metallocene prefer the same enantioface of the incoming monomer. With

Table 4
Unidirectional site epimerization model applied to **3**/MAO[a]

Entry	13		14		15		16		17		18	
	obs	calc	obs	calc	obs	calc	obs	calc	obs	calc	obs	calc
[*mmmm*]	26.4	26.8	26.0	26.8	27.2	28.0	28.4	30.4	34.2	35.4	40.1	40.7
[*mmmr*]	14.3	14.6	14.6	14.6	15.7	15.2	16.5	15.9	16.8	16.4	16.4	16.2
[*rmmr*]	6.5	4.8	5.9	4.8	4.5	4.1	3.7	3.3	2.9	2.3	3.0	1.8
[*mmrr*]	23.2	22.9	23.6	22.9	22.7	22.3	20.2	21.3	17.4	20.0	15.8	18.8
[*mmrm*] + [*rrmr*]	2.2	2.4	2.2	2.4	3.0	3.2	5.5	4.2	6.6	4.7	6.4	4.4
[*mrmr*]	0.6	1.2	0.6	1.2	0.6	1.2	1.2	1.2	2.7	1.1	2.1	1.1
[*rrrr*]	9.6	10.5	9.9	10.5	8.9	9.3	6.3	7.5	3.7	5.1	2.7	3.5
[*rrrm*]	9.0	9.6	9.1	9.6	8.2	9.1	7.7	8.1	5.8	6.3	4.8	4.9
[*mrrm*]	8.3	7.3	8.0	7.3	9.1	7.6	10.4	8.1	9.8	8.6	8.8	8.7
[*m*]	60.2	59.4	59.8	59.4	60.6	60.7	62.1	62.9	67.3	67.1	71.6	70.8
[*r*]	39.9	40.6	40.2	40.6	39.4	39.3	37.9	37.1	32.7	32.9	28.4	29.2
ε		0.000		0.000		0.069		0.180		0.354		0.485
RMS error		0.806		0.657		0.722		1.260		1.432		1.365

[a] The parameters α (0.974) and β (0.599) are determined by RMS minimization of entry 13 and are maintained at these values for application to entries 14–18.

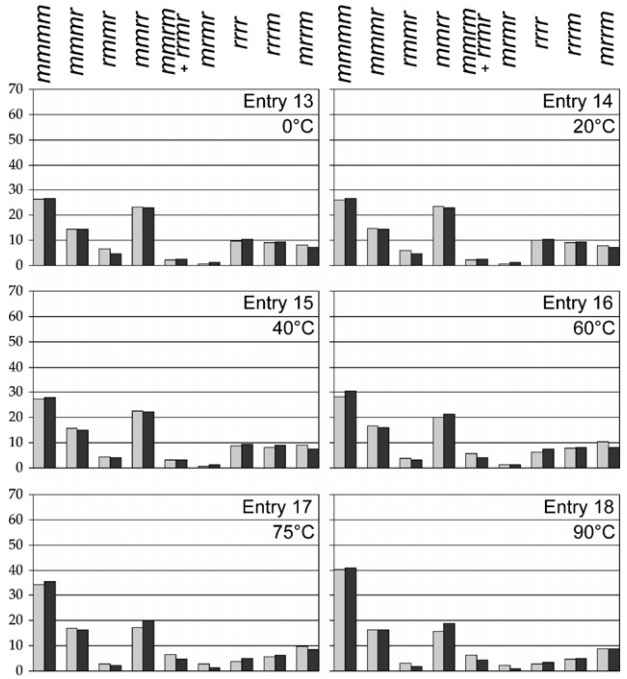

Fig. 9. Observed (light) vs. calculated (dark) pentad distributions for the unidirectional site epimerization model applied to **3**/MAO (Table 4, entries 13–18).

fixed values of α and β, conditions of dilute monomer (1.1 M), and increasing polymerization temperature (0, 20, 40, 60, 75, 90 °C) the unidirectional site epimerization parameter, ε, increases: 0.000, 0.000, 0.069, 0.180, 0.354, 0.485. Fig. 9 compares the observed and calculated pentad distributions with **3**/MAO and illustrates that this system is moderately responsive to changes that increase the likelihood of unimolecular site epimerization over that of bimolecular propagation. For this system with $[C_3H_6] = 1.1$ M and $T_p = 20$ °C, $\varepsilon = 0.000$; in contrast, for **1**/MAO and **2**/MAO under similar conditions ($[C_3H_6] = 0.8$ M, $T_p = 25$ °C), $\varepsilon = 0.910$ and 0.629, respectively.

The seemingly minor substitution of the isopropylidene bridge of **3** for the dimethylsilylene bridge of Me_2Si(3-(2-adamantyl)-C_5H_3)($C_{13}H_8$)$ZrCl_2$ (**4**) results in a drastically different polymerization behavior [17]. A least squares fit of the unidirectional model to entry 19 ($[C_3H_6] = 1.1$ M, $T_p = 0$ °C) provides the following parameters: $\alpha = 0.888$, $\beta = 0.872$, and $\varepsilon = 0.437$ (RMS error = 1.440). Although the extent of site epimerization for **3**/MAO under these conditions is negligible, **4**/MAO site epimerizes extensively. Thus, there is considerable uncertainty in the above calculated parameters for **4**/MAO and they are furthermore suspect because such C_1-symmetric catalysts do not usually exhibit congruent α and β parameters. Consequently, the stereochemical parameters from the isosteric catalyst **3**/MAO ($\alpha = 0.974$ and $\beta = 0.599$) are preferentially applied to **4**/MAO in the calculation of the corresponding ε values, which are reported in Table 5. Fig. 10 depicts the observed and calculated pentad distributions for **4**/MAO and confirms that they are consonant despite the application of α and β from **3**/MAO.

With fixed values of α and β, conditions of dilute monomer (1.1 M), and increasing polymerization temperature (0, 20, 40, 60, 80 °C) the unidirectional site epimerization parameter, ε, increases and then decreases for **4**/MAO: 0.709, 0.876, 0.913, 0.842, 0.792. The calculated decrease in ε with higher temperatures is inconsistent with the general observation that unimolecular reactions compete more effectively with bimolecular ones with increasing temperatures. The simplest explanation is that bidirectional site epimerization [12] engages above 40 °C. The decrease in isotacticity at higher temperatures is then rationalized because the less stereoselective site (site B) is increasingly employed. No sign of this unusual behavior is observed with **3**/MAO; a steady rise in ε and [*m*] is found with increasing polymerization temperature. Fig. 11 plots the unidirectional site epimerization parameter, ε, as a function of polymerization temperature for **3**/MAO and **4**/MAO with a monomer concentration of 1.1 M.

Table 5
Unidirectional site epimerization model applied to **4**/MAO[a]

Entry	19		20		21		22		23	
	obs	calc	obs	calc	obs	calc	obs	calc	obs	calc
[*mmmm*]	53.3	54.1	69.5	70.2	74.0	74.8	65.3	66.3	60.7	61.2
[*mmmr*]	12.4	14.3	10.0	10.4	6.5	9.0	10.4	11.4	12.8	12.7
[*rmmr*]	2.4	1.0	2.0	0.4	1.5	0.3	1.4	0.5	1.2	0.7
[*mmrr*]	12.7	15.5	8.9	10.7	9.3	9.1	9.0	11.9	11.4	13.5
[*mmrm*] + [*rrmr*]	7.0	2.9	2.3	1.3	2.3	1.0	4.0	1.6	4.2	2.1
[*mrmr*]	2.6	0.8	1.4	0.5	1.4	0.4	1.5	0.6	1.6	0.7
[*rrrr*]	1.1	1.4	0.5	0.5	0.9	0.3	1.2	0.6	0.8	0.9
[*rrrm*]	2.9	2.4	0.9	0.8	0.9	0.6	2.6	1.9	1.6	1.6
[*mrrm*]	5.5	7.6	4.3	5.3	3.2	4.6	4.6	5.7	5.8	6.7
[*m*]	79.3	79.0	87.8	87.2	88.5	89.3	84.4	85.3	83.3	82.7
[*r*]	20.7	21.0	12.0	12.8	11.5	10.7	15.6	14.7	16.8	17.3
ε		0.709		0.876		0.913		0.842		0.792
RMS error		2.084		1.007		1.220		1.565		1.095

[a] The parameters α (0.974) and β (0.599) are determined by RMS minimization of entry 13 (from **3**/MAO) and are maintained at these values for application to entries 19–23.

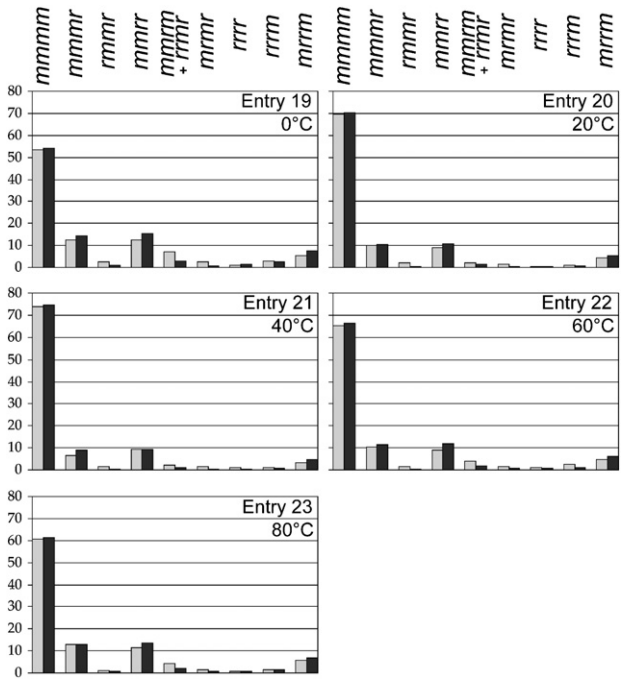

Fig. 10. Observed (light) vs. calculated (dark) pentad distributions for the unidirectional site epimerization model applied to **4**/MAO (Table 5, entries 19–23).

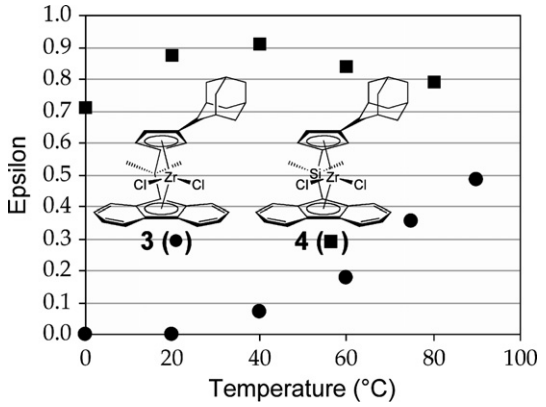

Fig. 11. The site epimerization parameter ε varies as a function of polymerization temperature for **3**/MAO (circles) and **4**/MAO (squares) for $[C_3H_6] = 1.1$ M.

3. Conclusions

A satisfactory stereochemical description of polypropylenes obtained with C_1-symmetric metallocenes **1**–**4**/MAO relies on the inclusion of the parameter ε, which quantifies the likelihood of unidirectional site epimerization, relative to propagation. Inclusion of this parameter—in addition to the enantiofacial selectivity parameters α and β—was necessary and sufficient since no evidence for site epimerization in the opposite direction was identified, except for **4**/MAO at higher temperatures. In general ε was found to increase with decreasing monomer concentration and increasing polymerization temperature—although the specific dependence is highly sensitive to the nature of the catalyst employed. The singly isopropylidene-bridged catalyst **3**/MAO was the least susceptible to site epimerization. A wide range of ε values was calculated for the doubly dimethylsilyl-bridged catalysts **1**/MAO and **2**/MAO, with the obtained value being highly dependent on the polymerization conditions. The singly dimethylsilyl-bridged metallocene **4**/MAO was the most susceptible to site epimerization and afforded large ε values under all polymerization conditions. For more complex polymerization systems, it may be necessary and instructive to apply more complex site epimerization models, including those that account for bidirectional site epimerization [3].

4. Experimental

4.1. Metallocene synthesis

Polypropylene pentad distribution data from **1**/MAO and **2**/MAO were obtained from the literature [4b]. Metallocene precatalysts **3** and **4** were synthesized according to reported methods [5a,11].

4.2. General polymerization procedure

Caution: All polymerization procedures should be performed behind a blast shield. All polymerization reactions were prepared in nitrogen filled gloveboxes. Methylaluminoxane (MAO) was purchased as a toluene solution from Albemarle Corporation and used as the dry powder obtained by *in vacuo* removal of all volatiles. Toluene was dried over sodium and distilled. Propylene from Scott Specialty Gases (>99.5%) was used following passage through a Matheson 6410 drying system equipped with an OXYSORB™ column. Polymerizations were conducted in a graduated Lab-Crest® (Andrews Glass) glass reaction vessel (3 oz. nominal volume) and were stirred with a magnetic stir bar. Monomer was condensed into the vessel (containing toluene and MAO) over several minutes at room temperature. The vessel was then equilibrated at the polymerization temperature with an ice or water bath for 10 min. A given reaction commenced upon injection of a toluene solution of the metallocene into the vessel with a 2.5 mL Hamilton syringe rated to 200 psi. Polymerization reactions were vented and quenched with a small volume of methanol/concentrated aqueous HCl (12:1) and the polymers were separated from hydrolyzed aluminoxanes by precipitation from methanol. Toluene and methanol were removed from the obtained polymers by *in vacuo* drying.

4.3. Representative polymerization procedures

4.3.1. Entry 13

In the glove box, a 3 oz. Lab Crest pressure reactor was charged with MAO (0.102 g, 1.76 mmol [Al], 2000 equiv.) and 28.0 mL toluene. Propylene (3 mL) was condensed in at room temperature and the vessel equilibrated at 0 °C for 10 min. A solution of Me_2C(3-(2-adamantyl)C_5H_3)

$(C_{13}H_8)ZrCl_2$ **3** (0.0005 g, 9×10^{-4} mmol) in toluene (2.0 mL) was injected and the reaction was stirred in a 0 °C ice/water bath for 30 min. The reaction was vented and quenched with methanol/aqueous HCl. 0.13 g of polypropylene were obtained. Reaction durations and isolated yields were as follows: Entry 14, 10 min, 0.25 g; entry 15, 10 min, 0.44 g; entry 16, 10 min, 0.18 g; entry 17, 30 min, 0.15 g; entry 18, 60 min, 0.21 g.

4.3.2. Entry 19

In the glove box, a 3 oz. Lab Crest pressure reactor was charged with MAO (0.100 g, 1.72 mmol [Al], 1000 equiv.) and 28.0 mL toluene. Propylene (3 mL) was condensed in at room temperature and the vessel equilibrated at 0 °C for 10 min. A solution of $Me_2Si(3\text{-}(2\text{-adamantyl})C_5H_3)(C_{13}H_8)ZrCl_2$ **4** (0.0010 g, 1.7×10^{-3} mmol) in toluene (2.0 mL) was injected and the reaction was stirred in a 0 °C ice/water bath for 90 min. The reaction was vented and quenched with methanol/aqueous HCl. 1.10 g of polypropylene were obtained. Reaction durations and isolated yields were as follows: Entry 20, 45 min, 1.07 g; entry 21, 15 min, 1.38 g; entry 22, 15 min, 1.54 g; entry 23, 15 min, 1.86 g.

4.4. Polymer characterization

Polymer melting temperatures were determined by differential scanning calorimetry (Perkin–Elmer DSC 7). The second scan (from 50 °C to 200 °C at 10 °C/min) was used when subsequent scans were similar. The polymer pentad distributions were determined by integration of the nine resolved peaks in the methyl region (19–22 ppm) of the ^{13}C NMR spectra obtained [14]. Spectra were acquired at 124 °C with tetrachloroethane-d_2 as solvent. A 90° pulse was employed with broadband decoupling. A delay time of 3 s and a minimum of 1000 scans were used.

Acknowledgments

This research is supported by grants from The Robert A. Welch Foundation (No. A-1537) and the Texas Advanced Technology Program (No. 010366-0196-2003). The National Science Foundation (CAREER CHE-0548197) is also graciously acknowledged for financial support.

Appendix A. Supplementary material

Additional details of the statistical model used to generate the graphical and tabular data. Supplementary data associated with this article can be found, in the online version, at doi:10.1016/j.jorganchem.2007.06.043.

References

[1] (a) For reviews and leading references, see: H.-H. Brintzinger, D. Fischer, R. Mülhaupt, B. Rieger, R.M. Waymouth, Angew. Chem., Intl. Ed. Engl. 34 (1995) 1143–1170;
(b) G. Fink, R. Mülhaupt, H.-H. Brintzinger (Eds.), Ziegler Catalysts, Recent Scientific Innovations and Technological Improvements, Springer, Berlin, 1995;
(c) W. Kaminsky, M. Arndt, Adv. Polym. Sci. 127 (1997) 143–187;
(d) C. Janiak, in: A. Togni, R.L. Halterman (Eds.), Metallocenes: Synthesis, Reactivity, Applications, Wiley-VCH, Weinheim, 1998, pp. 547–623;
(e) G.J.P. Britovsek, V.C. Gibson, D.F. Wass, Angew. Chem., Intl. Ed. Engl. 38 (1999) 429–447;
(f) G.W. Coates, Chem. Rev. 100 (2000) 1223–1252;
(g) L. Resconi, L. Cavallo, A. Fait, F. Piemontesi, Chem. Rev. 100 (2000) 1253–1345;
(h) G. Vlád, in: I.T. Horváth (Ed.), Encyclopedia of Catalysis, vol. 5, I, Wiley Interscience, Hoboken, New Jersey, 2003, pp. 611–737.
[2] (a) F.P. Price, in: G. Lowry (Ed.), Markov Chains and Monte Carlo Calculations in Polymer Science, Marcel Dekker, New York, 1970 (Chapter 7);
(b) F.A. Bovey, High Resolution NMR of Macromolecules, Academic Press, New York, 1972;
(c) J.C. Randall, Polymer Sequence Determination: Carbon-13 NMR Method, Academic Press, New York, 1977;
(d) M. Farina, Top. Stereochem. 17 (1987) 1–111;
(e) For leading references, see: J.C. Randall, Macromolecules 30 (1997) 803–816.
[3] V. Busico, R. Cipullo, Prog. Polym. Sci. 26 (2001) 443–533.
[4] (a) T.A. Herzog, D.L. Zubris, J.E. Bercaw, J. Am. Chem. Soc. 118 (1996) 11988–11989;
(b) D. Veghini, L. Henling, T. Burkhardt, J.E. Bercaw, J. Am. Chem. Soc. 121 (1999) 564–573;
(c) S. Miyake, J.E. Bercaw, J. Mol. Catal. A: Chem. 128 (1998) 29–39;
(d) D. Veghini, M.W. Day, J.E. Bercaw, Inorg. Chim. Acta 280 (1998) 226–232;
(e) F. Grisi, P. Longo, A. Zambelli, J.A. Ewen, J. Mol. Catal. A: Chem. 140 (1999) 225–233;
(f) B.L. Zhu, B.Q. Wang, S.S. Xu, X.Z. Zhou, Chin. J. Org. Chem. 23 (2003) 1049–1057;
(g) L. Cavallo, P. Corradini, G. Guerra, L. Resconi, Organometallics 15 (1996) 2254–2263.
[5] (a) S.A. Miller, Ph.D. Thesis in Chemistry, California Institute of Technology, 2000 (Chapter 2);
(b) S.A. Miller, J.E. Bercaw, Organometallics 21 (2002) 934–945;
(c) S.A. Miller, J.E. Bercaw, US Patent 6469188, 2002;
(d) S.A. Miller, J.E. Bercaw, US Patent 6693153, 2004.
[6] (a) M. Farina, G. Di Silvestro, P. Sozzani, Macromolecules 26 (1993) 946–950;
(b) M. Farina, A. Terragni, Makromol. Chem. Rapid. Commun. 14 (1993) 791–798;
(c) M. Farina, G. Di Silvestro, A. Terragni, Macromol. Chem. Phys. 196 (1995) 353–367;
(d) G. Di Silvestro, P. Sozzani, A. Terragni, Macromol. Chem. Phys. 197 (1996) 3209–3228.
[7] (a) W.J. Gauthier, S. Collins, Macromol. Symp. 98 (1995) 223–231;
(b) W.J. Gauthier, S. Collins, Macromolecules 28 (1995) 3779–3786;
(c) A.M. Bravakis, L.E. Bailey, M. Pigeon, S. Collins, Macromolecules 31 (1998) 1000–1009.
[8] (a) J.C. Randall, Macromolecules 30 (1997) 803–816;
(b) J.C. Randall, R.G. Alamo, P.K. Agarwal, C.J. Ruff, Macromolecules 36 (2003) 1572–1584.
[9] (a) M. Brookhart, M.L.H. Green, L.L. Wong, Prog. Inorg. Chem. 36 (1998) 1–124;
(b) M. Brookhart, M.L.H. Green, J. Organomet. Chem. 250 (1983) 395–408;
(c) Ref. [1d, p. 565].
[10] The term "site epimerization mechanism" is used in preference to other terms found in the literature: "consecutive addition" (Ref. [6b]); "skipped insertion" (J.A. Ewen, M.J. Elder, R.L. Jones, L. Haspeslagh, J.L. Atwood, S.G. Bott, K. Robinson,

Makromol. Chem. Macromol. Symp. 48/49 (1991) 253–295); "back-skip mechanism" (Ref. [17a]); "retention mechanism" ([6d]); and "isomerization without monomer insertion" (G. Fink, N. Herfert, Preprints of the International Symposium on Advances in Olefin, Cycloolefin, and Diolefin Polymerization, Lyon, 1992, p. 15).

[11] S.A. Miller, J.E. Bercaw, Organometallics 25 (2006) 3576–3592.

[12] Under a strict unidirectional site epimerization scenario, consecutive insertions at site B cannot occur. This would require the unfavorable migration of the polymer chain *toward* the bulky R substituent of the cyclopentadienyl ring.

[13] The least squares fit is calculated by RMS minimization of the nine resolved pentad intensities according to $(((\sum(I_{obs} - I_{calc})^2)/9)^{0.5}) = \text{RMS error}$.

[14] (a) V. Busico, R. Cipullo, P. Corradini, L. Landriani, M. Vacatello, A.L. Segre, Macromolecules 28 (1995) 1887–1892;
(b) V. Busico, R. Cipullo, G. Monaco, M. Vacatello, Macromolecules 30 (1997) 6251–6263.

[15] (a) V. Busico, R. Cipullo, J. Am. Chem. Soc. 116 (1994) 9329–9330;
(b) L. Resconi, A. Fait, F. Piemontesi, M. Colonnesi, H. Rychlicki, R. Zeigler, Macromolecules 28 (1995) 6667–6676;
(c) Ref. [1d, p. 596].

[16] A detailed analysis of the "allowed" pentads for **1**/MAO is presented in the Supplementary material of Ref. [4b].

[17] (a) Dimethylsilylene-bridged metallocene catalysts generally exhibit site epimerization that is competitive with insertion: J.A. Ewen, M.J. Elder, in: G. Fink, R. Mülhaupt, H.-H. Brintzinger (Eds.), Ziegler Catalysts, Recent Scientific Innovations and Technological Improvements, Springer, Berlin, 1995, pp. 99–109;
(b) W. Spaleck, M. Aulbach, B. Bachmann, F. Küber, A. Winter, Macromol. Symp. 89 (1995) 237–247;
(c) K. Patsidis, H.G. Alt, W. Milius, S.J. Palackal, J. Organomet. Chem. 509 (1996) 63–71.